The Journal of the Astronautical Sciences, Vol. 58, No. 2, April–June 2011, pp. 153–165

Earth Satellite Perturbation Theories as Approximate KAM Tori[1]

William E. Wiesel[2]

Abstract

Several standard Earth satellite general perturbation models can be converted into KAM tori, and are compared to KAM tori constructed from full geopotential integrations. Converting perturbation theories into tori allows absolute identification of spectral lines with the classical orbital elements. Comparisons are made of each torus representation against numerical integrations, and the torus spectra are also compared. The torus canonical coordinates Q_i are identified as the analogues of the "mean" mean anomaly $\bar{M}$, the longitude of the mean node $\bar{\Omega} - \theta_g$, and the mean argument of perigee $\bar{\omega}$. The associated torus canonical momenta P_i are approximately the usual Delaunay momenta. A norm on multiply-periodic functions allows the actual "distance" between perturbation theory tori and actual geopotential tori to be measured, and the frequency errors can be estimated. KAM tori and numerical integration can agree to meter level accuracy over time intervals of a decade.

Introduction

The KAM theorem has lain nearly unused for over a half century. Credited to Kolmogorov [1], Arnold [2], and Moser [3], the theorem states that Hamiltonian systems that are only a small perturbation away from a solvable system will have solutions which lie on tori. That is, they can be expressed as Fourier series in new coordinates Q_i which increment linearly with time at constant frequencies ω_i. Recently the current author has argued [4] that many, if not most Earth satellite orbits can be represented as KAM tori.

Of course, the major features of Earth satellite behavior are widely known. The oblateness of the Earth introduces precession of both the line of nodes and the line of apsides, so that the orbit can be thought of as a precessing ellipse. In this paper

[1]This paper is declared a work of the U.S. Government, and is not subject to copyright in the U.S.A. Opinions expressed are those of the author, and do not necessarily reflect those of the United States Air Force, the Department of Defense, or the U.S. Government.

[2]Professor, Astronautical Engineering; Department of Aeronautics and Astronautics, Air Force Institute of Technology, 2950 Hobson Way, Wright-Patterson AFB, OH 45433.

we will take common theories of satellite motion and convert them into the language of KAM tori. Although this will not produce the accuracy expected of a true KAM torus, it does produce both insight into the relationship between classical and KAM theories, as well as serving as an initial guess for converting classical orbital element sets into true KAM tori.

Conversely, we will find that a KAM torus contains within it the analogs of all of the familiar classical orbital elements. Methods will be developed to extract these quantities from the numerically fit torus.

Dynamics Models

In this section we will review the salient features of several approximate models for Earth satellite motion. Throughout this work, the effects of air drag and lunar and solar effects will be suppressed. The problem being considered is motion purely under the rotating non-point-mass gravitational field of the Earth.

The simplest model of Earth satellite motion would be the two-body problem. Although so inaccurate for low altitude satellites as to be useless for most purposes, note that this solution depends on three angles. The first, the mean anomaly M, has frequency $\dot{M} = \sqrt{\mu/a^3}$, the Keplerian frequency. Here a is the semimajor axis, and μ is the gravitational parameter. The other two angles, the node Ω and argument of perigee ω, are constant and therefore have zero frequencies. A system with only one frequency but $N \neq 1$ degrees of freedom is termed *totally degenerate.* But note that the solution is periodic in each of the three angles: M, Ω, and ω. That is, if two of these angles are held constant while the third is incremented by 2π, the position returns to the original value. Geometrically, this describes a torus.

Precessing Keplerian Ellipses

The earliest work on artificial satellites revealed that the oblateness of the Earth introduced secular terms in the motion of the node and the argument of perigee, whereas Kepler's third law was also modified. This breaks the degeneracy of the two-body problem, because there are now three separate frequencies

$$\dot{M} = \sqrt{\frac{\mu}{a^3}} - \frac{3\sqrt{\mu}J_2R_\oplus^2}{2a^{7/2}(1-e^2)^{3/2}}\left(\frac{3}{2}\sin^2 i - 1\right)$$

$$\dot{\Omega} = -\frac{3\sqrt{\mu}J_2R_\oplus^2}{2a^{7/2}(1-e^2)^2}\cos i$$

$$\dot{\omega} = -\frac{3\sqrt{\mu}J_2R_\oplus^2}{2a^{7/2}(1-e^2)^2}\left(\frac{5}{2}\sin^2 i - 2\right) \tag{1}$$

where e is the eccentricity, i the orbital inclination, $R_\oplus$ is the equatorial radius of the Earth, and J_2 the usual oblateness parameter. So a slightly better model than the two-body problem would be a precessing Keplerian ellipse. Notice that this is also multiply periodic in all three angles: M, Ω, and ω. If any two are held constant while the third is incremented by 2π, the position returns to its original value. Geometrically, this approximation is a torus. Rather than use this, proceed to a slightly better model in the next section.

The SGP4 Model

The SGP4 model, standing for "Simplified General Perturbations 4," has a long history. It is originally based on Brouwer's [5] 1959 theory of satellite motion perturbed by the Earth's zonal harmonics. Code for this model was first released by Hoots and Roehrich [6]. A history of changes and a very useful description of the content of the algorithms is by Hoots and Glover [7]. The Hoots and Roehrich fortran algorithm is the version of SGP4 we have used, in spite of the fact that more representative versions of the SGP4 algorithm are available from Vallado [8]. Thus, we make no claim that our SGP4 results are necessarily characteristic of current Spacetrack accuracy. The code produces position and velocity vectors at a given time from input mean elements, but only the position predictions have been used to fit tori in this paper.

Following the descriptions of Vallado and Hoots, we have removed the portions of the SGP4 algorithm that refer to air drag and lunar and solar perturbations, as well as long period resonant harmonics for so-called deep space satellites. What remains is the approximate perturbation solution for the zonal harmonic problem, including J_2, J_3, and J_4. This is then transformed to the Earth-centered rotating (ECR) frame, where the KAM torus is expected to exist. When this is done, it is found that the algorithm depends on three angles, the "mean" mean anomaly $\bar{M} = Q_1$, the longitude of the mean node $\bar{\Omega} - \theta_g = Q_2$, and the mean argument of perigee $\bar{\omega} = Q_3$. It is multiply periodic in all three of these angles, meaning that if any two are held constant and the third incremented by 2π, the algorithm returns to its original values. These three angles increment linearly with time, and time appears nowhere else in the algorithm once air drag and long period resonant effects are removed. That is, geometrically this solution is a torus.

KAM Tori

The KAM theorem, see e.g., Arnold [9], predicts that the solutions to lightly perturbed autonomous Hamiltonian systems will (mostly) lie on invariant tori. This has been applied to Earth satellites by Wiesel [4]. There it was argued that in order to obtain an autonomous dynamical system the problem should be posed in the Earth-centered rotating reference frame, giving a Hamiltonian of

$$\begin{aligned}\mathcal{H} = {} & \tfrac{1}{2}(p_x^2 + p_y^2 + p_z^2) + \omega_\oplus (y p_x - x p_y) \\ & - \frac{\mu}{r} \sum_{n=0}^{\infty} \sum_{m=0}^{n} \left(\frac{r}{R_\oplus}\right)^{-n} P_n^m(\sin\delta) \\ & \times (C_{nm}\cos m\lambda + S_{nm}\sin m\lambda)\end{aligned} \tag{2}$$

Here C_{nm}, S_{nm} are the field coefficients that describe the gravity model. The functions P_n^m are the associated Legendre functions, and the radius r, geocentric latitude δ, and east longitude λ are found from

$$r = \sqrt{x^2 + y^2 + z^2} \qquad \sin\delta = \frac{z}{\sqrt{x^2 + y^2}} \qquad \tan\lambda = \frac{y}{x} \tag{3}$$

The canonical momenta are

$$p_x = \dot{x} - \omega_\oplus y \qquad p_y = \dot{y} + \omega_\oplus x \qquad p_z = \dot{z} \tag{4}$$

TABLE 1. Orbit Initial Conditions

	x	y	z
Position, $R_\oplus$	−0.691868571562343	0.733130309616952	−0.456270004676488
Velocity, $R_\oplus$/TU	−0.602386773528478	−0.675993455650518	−0.287924635404537

NASA's EGM-96 gravity model [10] has been used in all integrations, truncated to order and degree $n, m \leq 20$.

There are two useful algorithms to construct a KAM torus from a numerical integration. Wiesel [4] used a least squares technique, fitting not only the torus Fourier series

$$\mathbf{r} = \sum_j \{\mathbf{C}_j \cos(\mathbf{j} \cdot \mathbf{Q}) + \mathbf{S}_j \sin(\mathbf{j} \cdot \mathbf{Q})\} \tag{5}$$

but its frequencies ω_i as well. The above (5) is a vector valued Fourier Series in three angles. The coefficients $\mathbf{C}_j$ and $\mathbf{S}_j$ are vectors, but the summation indices j_i are also conveniently written as a vector $\mathbf{j}$, as are the angles $\mathbf{Q}$. The arguments of the sine and cosine functions then become dot products.

The second method, due to Laskar [11, 12], uses an accelerated form of a finite Fourier transform to extract the system frequencies and the torus Fourier coefficients. Tori reported in this article were constructed via a modified Laskar method, Bordner and Wiesel [13]. This method identifies isolated clusters of spectral lines in the Fourier transform of a long numerical integration, and extracts both the system basis frequencies and Fourier series coefficients.

Torus Construction and Comparison

In this section we compare the SGP4 model and the KAM torus algorithms over the same numerically integrated trajectory. To be as unbiased as possible, the numerically integrated trajectory is taken as the baseline for all three methods, and the SGP4 model was least-squares fitted to the numerical integration before comparisons were made. One orbit in particular will be followed throughout this paper. This is a low eccentricity orbit $e = 0.05$ with a perigee altitude of 300 kilometers, and an inclination of 30 degrees. The remainder of the two-body orbital elements will be cited shortly in comparison tables, but the two-body orbital elements were used to construct the following initial conditions, shown in Table 1. Units are earth radii $R_\oplus = 6378.135$ km, and time units (TU), where one time unit is approximately 13.44686457 min.

Because the SGP4 model is cited with respect to an inertial frame, it must be transformed to the Earth-centered rotating frame for comparison to the KAM tori method. This merely requires using the longitude of the ascending node Ω-θ_g rather than the right ascension of the ascending node itself, where θ_g is the right ascension of the Greenwich meridian. The models were implemented to give position vectors $\mathbf{r}(\mathbf{Q})$ in the earth centered rotating (ECR) frame, and then these functions were developed as Fourier series by direct numerical quadratures for the Fourier coefficients

$$\mathbf{C}_0 = \frac{1}{(2\pi)^3}\int_0^{2\pi} \mathbf{r}(\mathbf{Q})\, d\mathbf{Q}$$

$$\mathbf{C}_\mathbf{j} = \frac{2}{(2\pi)^3}\int_0^{2\pi} \mathbf{r}(\mathbf{Q}) \cos(\mathbf{j}\cdot\mathbf{Q})\, d\mathbf{Q} \tag{6}$$

$$\mathbf{S}_\mathbf{j} = \frac{2}{(2\pi)^3}\int_0^{2\pi} \mathbf{r}(\mathbf{Q}) \sin(\mathbf{j}\cdot\mathbf{Q})\, d\mathbf{Q} \tag{7}$$

The factors of 2π are appropriate for a three-dimensional Fourier series. These coefficients can then be directly compared to the KAM method, as well as to the original numerically integrated trajectory. Because this is just a construction of the SGP4 torus by Fourier analysis, it was found that the torus and the SGP4 model code agreed to within double precision accuracy.

Comparison of tori is facilitated by noting that for vector-valued multiply periodic functions $\mathbf{f}(t) = \mathbf{f}(\mathbf{Q}(t))$ with N angles that

$$\|\mathbf{f}(t)\| = \left\{\frac{1}{(2\pi)^N}\int_0^{2\pi} \mathbf{f}(\mathbf{Q})\cdot\mathbf{f}(\mathbf{Q})\, d\mathbf{Q}\right\}^{1/2} = \left\{\|\mathbf{C}_0\|^2 + \frac{1}{2}\sum_\mathbf{j}(\|\mathbf{C}_\mathbf{j}\|^2 + \|\mathbf{S}_\mathbf{j}\|^2)\right\}^{1/2} \tag{8}$$

is a norm on the space of N dimensional multiply periodic functions. It satisfies all three properties required of a norm: it is zero if and only if $\mathbf{f} \equiv 0$, $\|k\mathbf{f}(t)\| = k\,\|\mathbf{f}(t)\|$ for scalar k, and $\|\mathbf{f}(t) + \mathbf{g}(t)\| \le \|\mathbf{f}(t)\| + \|\mathbf{g}(t)\|$. The first two properties are trivial to show, while the last follows easily from the Fourier series form of the norm using the equivalent result for the Euclidean norm. We will find this result useful in evaluating how successfully we have approximated KAM tori, and in quantifying the difference between tori from perturbation theories and those derived from full geopotential orbits.

Numerical Experiments

Using the SGP4 model, we have conducted a survey of nearly circular, low altitude orbits. Fig. 1 shows the approximate placement of most of the prominent spectral lines in the SGP4 model. What is new, different, and valuable about this effort is that performing Fourier analysis of the SGP4 model allows absolute identification of each spectral line in terms of its classical orbital element secular rate component. The three frequencies are given approximately by the J_2 angular rates, but with respect to the Earth-centered rotating frame. They are

$$\omega_1 \approx \dot{M} \qquad \omega_2 \approx -\omega_\oplus + \dot{\Omega} \qquad \omega_3 \approx \dot{\omega} \tag{9}$$

Lines in Fig. 1 are labeled with the integer multiples n_i of the basis frequencies in combination $\omega = n_1\omega_1 + n_2\omega_2 + n_3\omega_3$. In particular, the contribution of the argument of perigee has been difficult to discern for small eccentricity orbits in our earlier efforts. It is always the smallest frequency of the three, often by a substantial factor. Because both Laskar Fourier spectral methods and least squares fitting

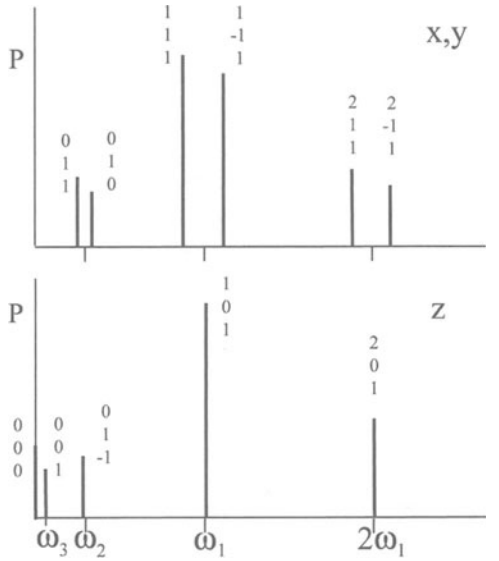

FIG. 1. Sketch of Important Spectral Lines in the SGP4 Model.

depend on a long arc of numerically integrated trajectory, the contribution of the classical argument of perigee has been hard to extract. But because the SGP4 tori are constructed by directly calculating the theories' Fourier coefficients, this contribution can be extracted without any significant error.

Figure 2 contrasts the Fourier power spectrum $P(\omega)$ of an orbit modeled by SGP4 with the equivalent spectra obtained from a full 20 by 20 geopotential numerical integration over approximately one year. The spectra of the full geopotential orbit is much richer, but at a given accuracy level it is finite. The

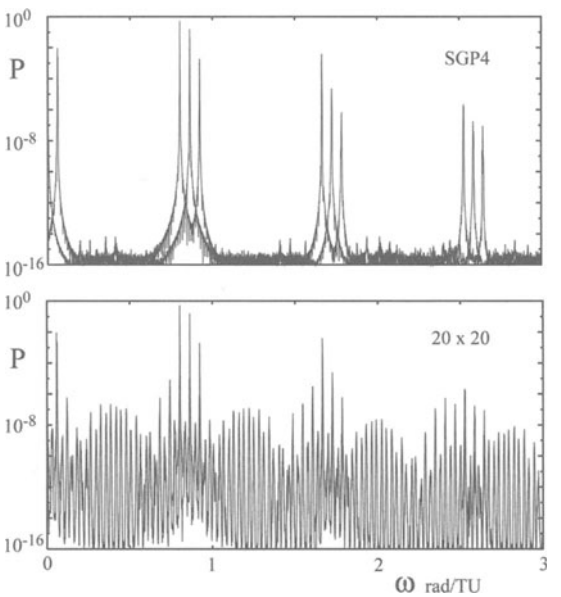

FIG. 2. Power Spectra of a Low Altitude Satellite Orbit Over about 1 Year, Using SGP4 (above) and a 20th by 20th Order Geopotential Integration (below).

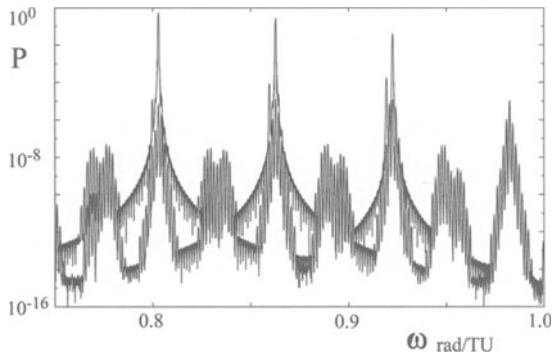

FIG. 3. Detail of the Power Spectra of the 20th Order Integration in the Region Around the Keplerian Frequency.

identification of the most prominant lines in the SGP4 spectrum makes it possible to extend this identification to the spectra of realistic orbits. In particular, the most prominent peaks are easily identified, and determining their frequencies allows construction of the torus basis frequency set to very high accuracy. We have used the 1, –, – and 2, –, – lines from the x, y, and z coordinates to construct such basis frequency sets without having to search directly for hard to find spectral lines.

There is still more detail not visible in Fig. 2. The region around the Keplerian orbital frequency ω_1 is shown enlarged in Fig. 3. The large central peak at $\omega \approx 0.87$ is from the z coordinate, and is closest to ω_1. It is flanked by large peaks from the x and y coordinates. These are the 1, 1, 1 and 1, -1, 1 features from the schematic spectra Fig. 1. They are essentially separated from the z coordinate peak by ω_2, which itself is very close to the rotational frequency of the earth. The flanks of the major peaks show considerable structure, which is of two types. The broader, more rounded sub-peaks are sidelobes of the finite Fourier transform used in these calculations, and are an artifact of the finite time limit employed. The sharper sub peaks, more closely spaced, are the argument of perigee frequency structures, and their spacing is the third frequency ω_3. It is these isolated clusters of spectral lines that the Bordner [13] modification to the Laskar algorithm finds and fits.

Finally, note that the power spectra reported in our original article [4] have far less detail, because they were much lower eccentricity orbits. This work has deliberately picked an orbital eccentricity $e = 0.05$, which has a much more dramatic frequency spectrum.

The Action Momenta and Angular Variables

Having an expression for the position of the satellite on the torus does not specify the full orbital state. The velocity vector, or equivalently the canonical momenta are needed, both in the "native" Earth-centered rotating frame, and in the canonical variables on the torus itself. Then, the action momenta P_i conjugate to the torus angle coordinates Q_i can be found by calculating

$$P_i = \frac{1}{2\pi}\oint_{\Gamma_i} \mathbf{p} \cdot \mathrm{d}\mathbf{q} = \frac{1}{2\pi}\int_0^{2\pi} \mathbf{p} \cdot \frac{\partial \mathbf{q}}{\partial Q_i}\,\mathrm{d}Q_i \tag{10}$$

Here, $\mathbf{q}$ is the vector of rectangular coordinates, $\mathbf{p}$ is the vector of physical momenta (4), and Γ_i is one of the fundamental contours around the torus. These can

be found by taking the native coordinate expression $\mathbf{q}(\mathbf{Q})$ in terms of the new coordinates, and integrating along one coordinate direction dQ_i while holding all of the other Q_i constant. With both the native coordinate vector $\mathbf{q}$ and the native momentum vector $\mathbf{p}$ expressed as truncated Fourier series, the calculation sketched above in (10) is quite possible using numerical quadratures.

If the rotation rate of the Earth is set to zero in the above, and the gravity field is restricted to the Newtonian point mass term, then we recover the two-body problem. In this case the action integrals above return the well known Delaunay momenta

$$P_1 = L = \sqrt{\mu a} \qquad P_2 = H = \sqrt{\mu a}\sqrt{1-e^2}\cos i \qquad P_3 = G = \sqrt{\mu a}\sqrt{1-e^2} \tag{11}$$

This is, however, mostly a check on the code, since we are not producing action angle variables for the two-body problem. The two-body problem coordinates are changed from the Delaunay coordinates $l = M$, $g = \omega$, and $h = \Omega$ to the effective Earth-centered rotating torus coordinates

$$Q_1 = l = M \qquad Q_2 = \Omega - \omega_\oplus t = h - \omega_\oplus t \qquad Q_3 = \omega = g \tag{12}$$

by using the F_2 generating function

$$F_2 = P_1 l + P_2(h - \omega_\oplus t) + P_3 g \tag{13}$$

This will then give the new momenta in the ECR frame as

$$L = \frac{\partial F_2}{\partial l} = P_1 \qquad H = \frac{\partial F_2}{\partial h} = P_2 \qquad G = \frac{\partial F_2}{\partial g} = P_3 \tag{14}$$

That is, the momenta for the two-body problem in the ECR frame are still the Delaunay momenta. The numbering has been changed to put the variables in decreasing order of frequency, with ω_1 the largest frequency, and ω_3, essentially the argument of perigee secular rate, the lowest. Using (10), these momenta can be calculated for any of the tori constructed here, using any of the dynamics models.

Then using the usual expression for the J_2 secular rates, and remembering to add the two-body term and the $\partial F_2/\partial t$ term, the approximate Hamiltonian function on the torus, in torus variables, becomes

$$\mathcal{K} = -\frac{\mu^2}{2P_1^2} - P_2\omega_\oplus + \frac{\mu^4 J_2 R_\oplus^2}{4P_1^3 P_3^3} - \frac{3\mu^4 J_2 R_\oplus^2 P_2^2}{4P_1^3 P_3^5} \tag{15}$$

In this form, the momenta are obviously constant, and the coordinates have the (approximate) constant frequencies cited earlier. Both the SGP4 model and the KAM torus model, of course, go beyond this approximation.

We have argued that the torus coordinates Q_i can be identified with the mean anomaly, the longitude of the node, and the argument of perigee. Hence it is not surprising to find that their conjugate momenta are the Delaunay momenta associated with these variables. However, can the torus angles be permuted to make them more like the classical angles? The answer is yes.

The usual torus construction algorithms simply place the origin $Q_i = 0$ at the epoch time of the data. Since these angles are linear in time, we are free to add a phase variable

$$Q_i = Q_i(t_0) + \omega_i(t - t_0) \tag{16}$$

TABLE 2. Orbit Frequencies, rad/TU

Dynamics Model	ω_1	ω_2	ω_3
TBP	0.86115914723	−0.058833592	0
SGP4	0.861158955581817	−0.05983288855038447	0.001586399545565241
Torus	0.861159538493074	−0.05983301222000043	0.001585676087872301

to more nearly align with their classical definitions. Given the torus Fourier series, this can be done as a three step process. First, holding Q_2 and Q_3 at zero, the value of Q_1 can be adjusted to minimize the radius vector in the range $0 \leq Q_1 \leq 2\pi$. This places the origin of Q_1, the mean-anomaly analog, at perigee. Then, holding Q_1 at perigee, and holding the longitude of the node Q_2 constant, the value of Q_3 is found that places the satellite on the equator crossing from south to north. This sets the argument of perigee analog's origin at the ascending node. Finally, with the origins of Q_1 and Q_3 identified, the origin of the longitude of the ascending node is adjusted to place the node on the Greenwich meridian. This sets the origin of the torus coordinates Q_i at the closest analog values to their classical two-body element counterparts.

A Sample Case

In this section we will compare orbital fits for both an SGP4 torus and a KAM torus for the orbit cited earlier in Table 1. Each model produces its own set of frequencies, which are compared in Table 2. Although the two-body problem (TBP) nominally only has one frequency, the Keplerian mean motion, in the Earth-centered rotating frame the node will regress with the rotation rate of the Earth, and this is indicated in the table. The SGP4 model was fit to a two week arc of numerically integrated trajectory, using the geopotential through order and degree twenty. The SGP4 model uses secular rates up through terms of order J_2^2 and J_4, so these differ from the pure two-body problem frequencies. Finally the KAM torus uses a set of basis frequencies fit, as indicated earlier, to the most prominent spectral lines in the Fourier transform of the orbit. These three frequencies were determined from 10 spectral lines by a least squares fit, with errors from the fit being approximately one part in 10^{13}. There is quite good agreement between the SGP4 frequencies and the KAM torus frequencies, although the latter is based on the entire geopotential through order twenty, and had the (perhaps unfair) advantage of being based on a one-year integration.

Table 3 shows the momenta for each of the three models. Of course, the two-body problem merely cites the Delaunay momenta determined from the classical orbital elements. These are in close agreement with the equivalent

TABLE 3. Orbit Momenta

Dynamics Model	$P_1 = L$	$P_2 = H$	$P_3 = G$
TBP	1.0510874734	0.9091365593	1.04978052722
SGP4	1.05138476567018	0.909355469002676	1.04999414340781
Torus	1.05137969328809	0.909316594845978	1.05007500771064

TABLE 4. Orbit Phase Angles, rad

Dynamics Model	$Q_1 = M_0$	$Q_2 = \Omega$	$Q_3 = \omega$
TBP	1.54321	4.5678	2.46810
SGP4	1.5486633937382	4.56742583816523	2.46264247288152
Torus	1.55963981580271	4.56752444890610	2.44933405414877

momenta calculated numerically from both the SGP4 torus and the KAM torus via equations (10). These integrations across the torus are theoretically independent of the values of the coordinates Q_j which are being held constant during integration around a fundamental contour Γ_i. This invariance was checked to double precision accuracy, in effect showing that both the SGP4 torus and the KAM torus constructed are canonical. It could be argued that knowing the Delaunay momenta analogues for the KAM torus, that these could be inverted to define a KAM torus semimajor axis, inclination, and eccentricity. We have resisted that temptation.

Finally, possessing both the KAM torus and the SGP4 torus, the orbital phase angles can be extracted as detailed in the previous section. These are shown in Table 4. The two-body values are just the classical orbital elements, and for our reference orbit were chosen to have the simple digit progressions shown in the table, when expressed in radians. For the SGP4 torus the "mean" mean elements agree with the values extracted from the torus representation of the SGP4 model, so there is no difference here. Phase angles extracted from the KAM torus are in quite close agreement with the earlier values, so once again the KAM model permits us to define angle variables that are analogous to the mean anomaly at epoch, the longitude of the node, and the argument of perigee.

There are two further ways to compare the SGP4 torus and the KAM torus to the actual solution, where the "actual" solution is taken to be the numerically integrated orbit. Fig. 4 shows the error in the position vectors predicted from the torus, compared to the numerically integrated values. Both show linear drift from

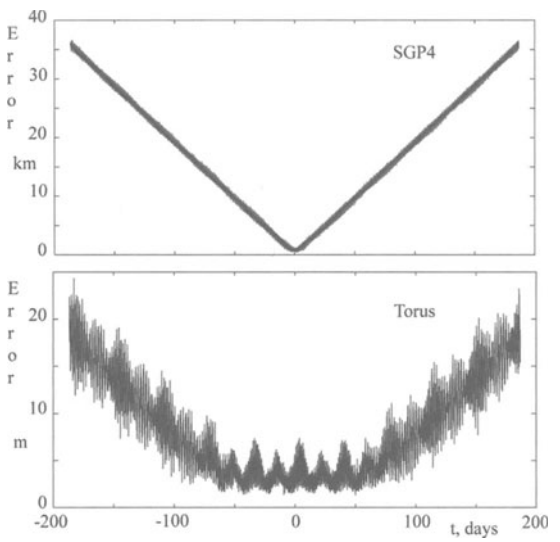

FIG. 4. Error Buildup Over 1 Year for the SGP4 Orbit (above) and the Torus (below).

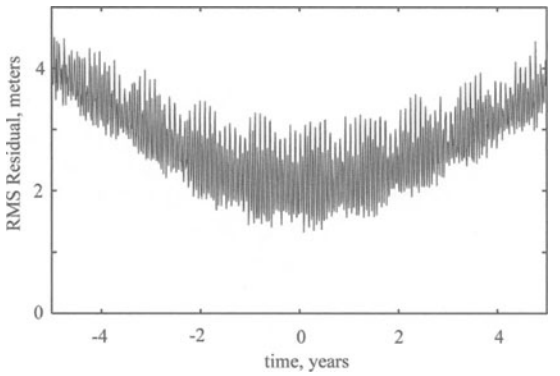

FIG. 5. Ten Year RMS Residuals, When the Torus Coordinates Q_i are Calculated in Extended Precision Arithmetic.

the numerically integrated solution. If this is interpreted as an in-track frequency error, the SGP4 torus is in error by $\delta\omega_{\text{sgp4}} \approx 3 \times 10^{-7}$. Similarly, the KAM torus seems to have a frequency error that is on the order of $\delta\omega_{\text{torus}} \approx 2 \times 10^{-10}$ radians/TU, but we will see the actual interpretation of this error shortly. Note the difference between the scales of the two plots: the SGP4 plot is in kilometers, while the KAM torus plot is in terms of meters of error.

However, besides the usual comparison of orbital solutions in the time domain, the fact that these are both tori makes it possible to compare the SGP4 torus to the KAM torus in the spatial domain. Taking the norm of the difference of the two tori via (8), the SGP4 and KAM tori differ by 0.9715 km. This is in the sense of a root-mean-square position difference between the two models, and this sets, in effect, an accuracy ceiling for the SGP4 model. Even if it had the correct orbital frequencies, the SGP4 model will differ (for this orbit) from reality by about one kilometer. The use of the norm allows this separation of geometric error from frequency error.

But the center interval of approximately ± 50 days in Fig. 4 for the KAM torus case is also of interest. At meter level error, there is a time t at which the accuracy of the phase calculation for each coordinate $Q_i = \omega_i t$ begins to degrade, as the subtraction of a large number of whole revolutions exceeds the accuracy available in double precision arithmetic. This point may have been reached here, and the resulting drift may only begin after an effective loss of double precision accuracy. This led the author to reprogram the calculation of the torus coordinates $Q_i = \omega_i t$ and their reduction modulo 2π in multiple precision arithmetic. This showed that the suspicion that double precision was insufficiently accurate was correct. Fig. 5 shows that the actual deviation between the numerical integration and the constructed KAM torus remains within a few meters over a decade. This, in spite of the fact that the KAM torus was constructed over only the central one-year time interval. The author makes no claim that an *actual* satellite orbit could be predicted to this accuracy for a decade, but merely notes that this is strong evidence for both the correctness of KAM theory, and the accuracy of numerical integration.

Discussion and Conclusions

In this article the two-body problem and the widely used SGP4 model of Earth satellite motion have been discussed in terms of KAM torus theory, and compared

with an actual KAM torus fit to a numerically integrated orbit. It was found that both the two-body problem and the SGP4 models are, in reality, torus models. But for the KAM torus, it was found that analogues of all of the classical orbital elements can be defined and numerically calculated from a high accuracy KAM torus fit to a trajectory.

In one sense, this is not surprising, since both models are endeavoring to describe the same physical reality. The KAM torus model, however, holds the promise of being able to represent the motion in the Earth's gravity field to an accuracy that is comparable to the accuracy of the numerical integration itself.

This paper shows that a KAM torus is in many ways the analog of a full analytic perturbation theory for Earth orbits. There are, however, two significant differences. First, the frequencies are obtained to very high accuracy, and not approximated by the perturbation series expansions. And secondly, the entire process is carried out numerically, not analytically.

The biggest drawbacks so far in constructing Earth orbit KAM tori has proven to be the reliance on a long numerical integration from which to extract the torus, either by least squares fitting, or by the Laskar spectral analysis technique. The argument of perigee rate in particular is difficult to observe, especially close to the critical inclination or at large distances from the earth. Alternate methods of torus construction is an active area of research. The comparison of the numerical integration and the KAM torus over one decade presents very, very strong evidence that some, if not most, purely gravitational trajectories about the Earth are KAM tori.

References

[1] KOLMOGOROV, A. "On the Conservation of Conditionally Periodic Motions under Small Perturbations of the Hamiltonian," *Doklady Akademii Nauk SSSR*, Vol. 98, January 1954, pp. 527–530.

[2] ARNOLD, V. "Proof of Kolmogorov's Theorem on the Preservation of Quasi-Periodic Motions under Small Perturbations of the Hamiltonian," *Russian Mathematical Survey*, Vol. 18, No. N6, 1963, pp. 9–36.

[3] MOSER, J. "On Invariant Curves of an Area Preserving Mapping of an Annulus," *Nachrichten der Akademie der Wissenschaften in Göttingen, II, Mathematisch-Physikalische Klasse,* Vol. Kl. IIa, January 1962, pp. 1–20.

[4] WIESEL, W.E. "Earth Satellite Orbits as KAM Tori," *The Journal of the Astronautical Sciences*, Vol. 56, April-June 2008, pp. 151–162.

[5] BROUWER, D. "Solution of the Problem of Artificial Satellite Theory Without Drag," *Astronomical Journal,* Vol. 64, No. 1274, 1959, pp. 378–396.

[6] HOOTS, F.R. and ROEHRICH, R.L. "Models for Propagation of the NORAD Element Sets," tech. rep., Project Spacetrack Report 3, U.S. Air Force Aerospace Defense Command, Colorado Springs, CO, Dec. 1980.

[7] HOOTS, F.R., SCHUMACHER, P.W., and GLOVER, R.A. "History of Analytical Orbit Modeling in the U.S. Space Surveillance System," *Journal of Guidance, Control and Dynamics,* Vol. 27, March-April 2004, pp. 174–185.

[8] VALLADO, D., CRAWFORD, P., HUJSAK, R., and KELSO, T.S. "Revisiting Spacetrack Report No.3," presented as paper AIAA 2006-6753 at the 2006 AIAA/AAS Astrodynamics Specialist Conference, 2006, pp. 1–88.

[9] ARNOLD, V.I. *Mathematical Methods of Classical Mechanics*, Springer-Verlag, New York, 1989.

[10] LEMOINE, F.G., KENYON, S.C., FACTOR, J.K., TRIMMER, R.G., PAVLIS, N.K., et al. "The Development of the Joint NASA, GSFC and NIMA Geopotential Model EGM96," *NASA/TP-1998-206861,* January 1998.

[11] LASKAR, J. "Introduction to Frequency Map Analysis," *Hamiltonian Systems with Three or More Degrees of Freedom*, C. Simo, ed., Springer-Verlag, New York, 1999, pp. 134–150.

[12] LASKAR, J. "Frequency Map Analysis and Quasiperiodic Decompositions," *Proceedings of Proquerolles School,* Sept 2001, pp. 1–31.

[13] BORDNER, R.E. and WIESEL, W.E. "Spectral Decomposition of Orbital Tori," *Journal of Guidance, Control, and Dynamics,* Vol. 34, No. 2, 2011, pp. 504–512.